chemistry proceedings

MDPI

Proceeding Paper

Synthesis and Characterization of a Dansyl-Based Fluorescent Probe for Analytical Purposes †

Jesús Sanmartín-Matalobos [1,*], Pilar Bermejo-Barrera [2], Yeneva Alves-Iglesias [1,2], Ana M. García-Deibe [1] and Matilde Fondo [1]

[1] Coordination and Supramolecular Chemistry Group (Suprametal), Institute of Materials (iMATUS), Department of Inorganic Chemistry, Faculty of Chemistry, Universidade de Santiago de Compostela, Avenida das Ciencias s/n, 15782 Santiago de Compostela, Spain; yeneva.alves.iglesias@usc.es (Y.A.-I.); ana.garcia.deibe@usc.es (A.M.G.-D.); matilde.fondo@usc.es (M.F.)

[2] Trace Element, Speciation and Spectroscopy Group (GETEE), Institute of Materials (iMATUS), Department of Analytical Chemistry, Nutrition and Bromatology, Faculty of Chemistry, Universidade de Santiago de Compostela, Avenida das Ciencias, s/n, 15782 Santiago de Compostela, Spain; pilar.bermejo@usc.es

* Correspondence: jesus.sanmartin@usc.es

† Presented at the 25th International Electronic Conference on Synthetic Organic Chemistry, 15–30 November 2021; Available online: https://ecsoc-25.sciforum.net/.

Abstract: With the aim of investigating the development of an easily synthesized dansyl-based fluorescent probe for detecting heavy-metal-based nanomaterials in aqueous solution, we synthetized and characterized a Schiff-base ligand, which we named H_3L. It was derived from the reaction of 4-formyl-3-hydroxybenzoic acid with *N*-(2-aminobenzyl)-5-(dimethylamino)naphthalene-1-sulfonamide. H_3L incorporates a suitable *O*,*N*-binding domain that can bind heavy-metal ions at the surface of the nanoparticles.

Keywords: Schiff base; fluorescent probes; NMR spectroscopy; UV–Vis spectroscopy

Citation: Sanmartín-Matalobos, J.; Bermejo-Barrera, P.; Alves-Iglesias, Y.; García-Deibe, A.M.; Fondo, M. Synthesis and Characterization of a Dansyl-Based Fluorescent Probe for Analytical Purposes. *Chem. Proc.* **2022**, *8*, 76. https://doi.org/10.3390/ecsoc-25-11775

Academic Editor: Julio A. Seijas

Published: 14 November 2021

1. Introduction

Human and environmental health risks of heavy-metal-based nanomaterials necessitate affordable and reliable techniques for their detection [1–4]. This would increase safety related to the handling and release into the environment of metal-based nanomaterials. Due to their selectivity, sensitivity and simplicity, chemical sensors such as fluorescent probes are very promising methods to be used not only for detection, but for quantification as well. Some optical sensors have been developed for the detection of Ag NPs [5–7], but investigation of fluorescent sensors to detect and quantify CuO NPs remains virtually unexplored. Recently, we have explored the chelating potential of two easily synthesized Schiff bases for CuO-NP sensing [8,9]. Now, we chose for our investigation the Schiff base H_3L, which derives from the reaction of 2-(aminomethyl)aniline with tosyl chloride and 4-formyl-3-hydroxybenzoic acid (Figure 1).

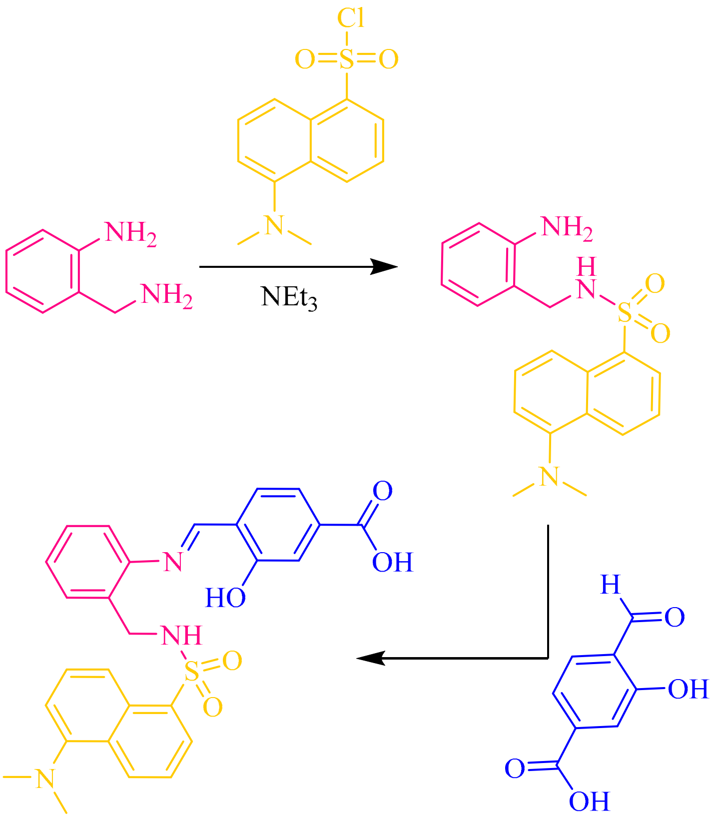

Figure 1. Schematic representation of the synthesis of H_3L in two steps: (i) selective dansylation of a primary diamine and (ii) aldiminic condensation of *N*-(2-aminobenzyl)-5-(dimethylamino)naphthalene-1-sulfonamide with 4-formyl-3-hydroxybenzoic acid.

2. Results and Discussion

H_3L can be obtained in a quick two-step synthesis. In the first step, 2-(aminomethyl) aniline reacts selectively through the aminomethyl group with dansyl chloride to form *N*-(2-aminobenzyl)-5-(dimethylamino)naphthalene-1-sulfonamide. The subsequent nucleophilic addition of *N*-(2-aminobenzyl)-5-(dimethylamino)naphthalene-1-sulfonamide to 4-formyl-3-hydroxybenzoic acid yields the desired Schiff-base ligand H_3L (Figure 1). The obtaining of H_3L was demonstrated using FT-IR, UV–Vis and NMR spectroscopies.

The most characteristic infrared bands of H_3L, such as ν N-H, ν C=O, ν C=N, ν_{as} OSO and ν_s OSO are highlighted in Figure 2, top. The infrared spectrum of H_3L unequivocally exhibits two new strong sharp bands at about 1613 and 1686 cm^{-1}, which are attributable to the formation of the imino group, and to the presence of the carboxylic-acid group, respectively. Infrared spectroscopy also evidenced the absence of three bands at about 1632, 3383 and 3472 cm^{-1}, which were attributed to δ HNH, ν_s HNH and ν_{as} HNH modes, respectively, in the spectrum of *N*-(2-aminobenzyl)-5-(dimethylamino)naphthalene-1-sulfonamide (Figure 2, bottom). Consequently, infrared spectroscopy provides strong evidence of the condensation of 4-formyl-3-hydroxybenzoic acid with *N*-(2-aminobenzyl)-5-(dimethylamino)naphthalene-1-sulfonamide through its non-dansylated amino group.

Figure 3 shows the ^{1}H-NMR spectra of H_3L (top) and *N*-(2-aminobenzyl)-5-(dimethylamino)naphthalene-1-sulfonamide (bottom), with signal assignment on a 3D model of each molecule. The most remarkable observation in the ^{1}H-NMR spectrum of H_3L is the presence of the imine proton at about 8.0 ppm (singlet) and the disappearance at 3.9 ppm of the amino group of *N*-(2-aminobenzyl)-5-(dimethylamino)naphthalene-1-sulfonamide. This is clear evidence of the condensation of *N*-(2-aminobenzyl)-5-(dimethylamino)naphthalene-1-sulfonamide with 4-formyl-3-hydroxybenzoic acid yielding the desired Schiff-base ligand H_3L. Thus, NMR spectroscopy supported the obtaining of H_3L. The most remarkable signals in the ^{1}H-NMR spectrum of *N*-(2-aminobenzyl)-5-

(dimethylamino)naphthalene-1-sulfonamide are those corresponding to methylene (doublet), amine (singlet) and sulfonamide (triplet) protons. The observation of these three signals is clear evidence of the selective dansylation of the aminomethyl group during the first step of the synthesis.

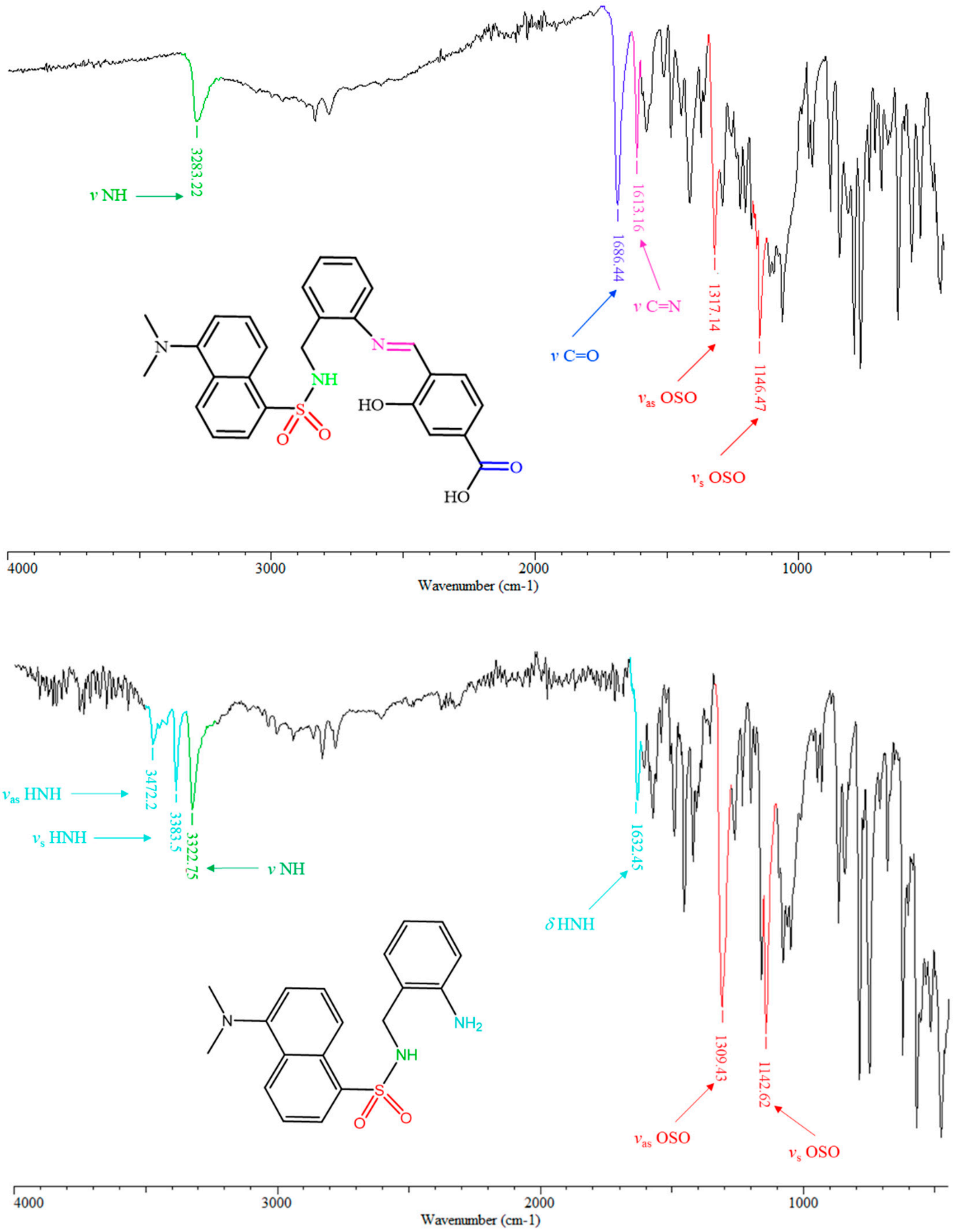

Figure 2. View of the ATR-IR spectra of H_3L (**top**) and *N*-(2-aminobenzyl)-5-(dimethylamino) naphthalene-1-sulfonamide (**bottom**), with signal assignment of remarkable functional groups of the molecules on the corresponding schemes.

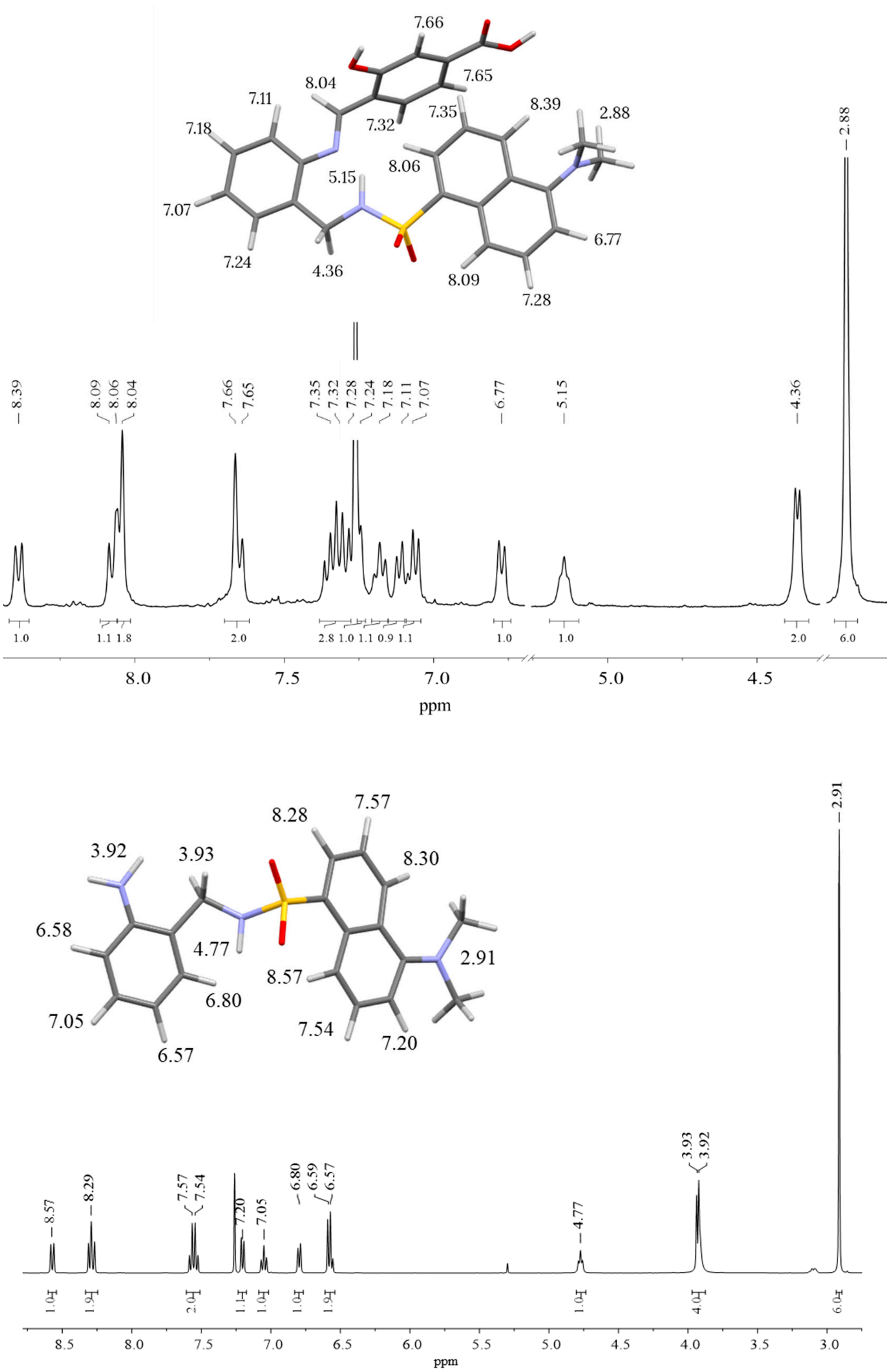

Figure 3. ^{1}H-NMR spectra (in chloroform-d) of H_3L (**top**) and *N*-(2-aminobenzyl)-5-(dimethylamino) naphthalene-1-sulfonamide (**bottom**), with signal assignment on a 3D model of each molecule.

H_3L displayed three intense intraligand absorption bands centered at about 225, 250 and 345 nm (Figure 4), corresponding to the π→π* and n→π* transitions of the conjugated system. The absorption band at about 225 nm is in accordance with the presence of the carboxyl group. The observation of two bands with maxima at about 250 and 345 nm evidenced the absorption behavior of the dansyl moiety [10]. The shoulder at about 265 nm can be attributed to the imino group [11] of H_3L.

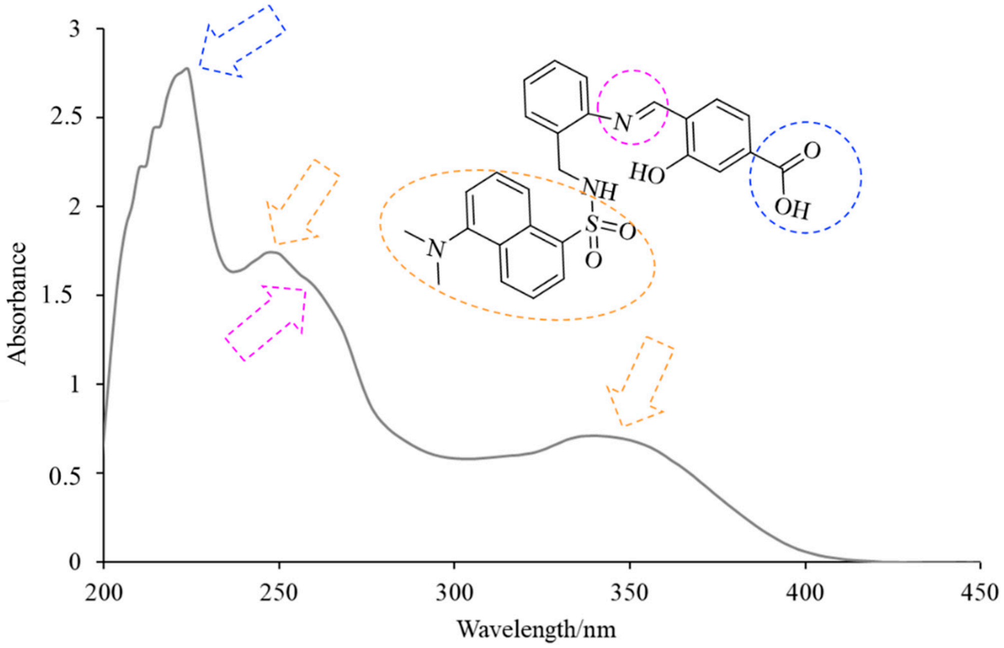

Figure 4. View of the UV–Vis spectrum of H_3L in ethanol solution.

An ethanol solution of H_3L emitted a maximal green fluorescence at 520 nm when it was exposed to visible light with a wavelength of 400 nm. The fluorescence behavior could be assigned to the dansyl moiety, which is known for the typical charged-transfer band between the donor dimethylamino group and the sulfonyl unit, centered around λ_{em} = 520 nm, as previously described [10]. The study of the influence of pH on the fluorescence spectrum of H_3L (Figure 5) showed that pH values of about 6 (and lower) resulted in protonation of the dimethylamino group, pH values of about 8 led to deprotonation of the carboxylic-acid group, but when the pH was about 9, deprotonation of the phenol group was achieved, and pH values of 11 led to deprotonation of the sulfonamide group. Therefore, varying the pH of the medium, the Schiff-base ligand can achieve different forms, such as H_4L^+, H_3L, H_2L^-, HL^{2-} and L^{3-}, with the anionic forms being the most emissive.

Preliminary studies showed that a pH value of about 12 favors the interaction between H_3L and CuO nanomaterials. This was evidenced by a pronounced decrease in the fluorescence intensity of an ethanol solution of H_3L when CuO was added in increasing amounts. Figure 6 shows the gradual quenching of the fluorescence intensity of an ethanol solution of H_3L after the addition of CuO nanopowder.

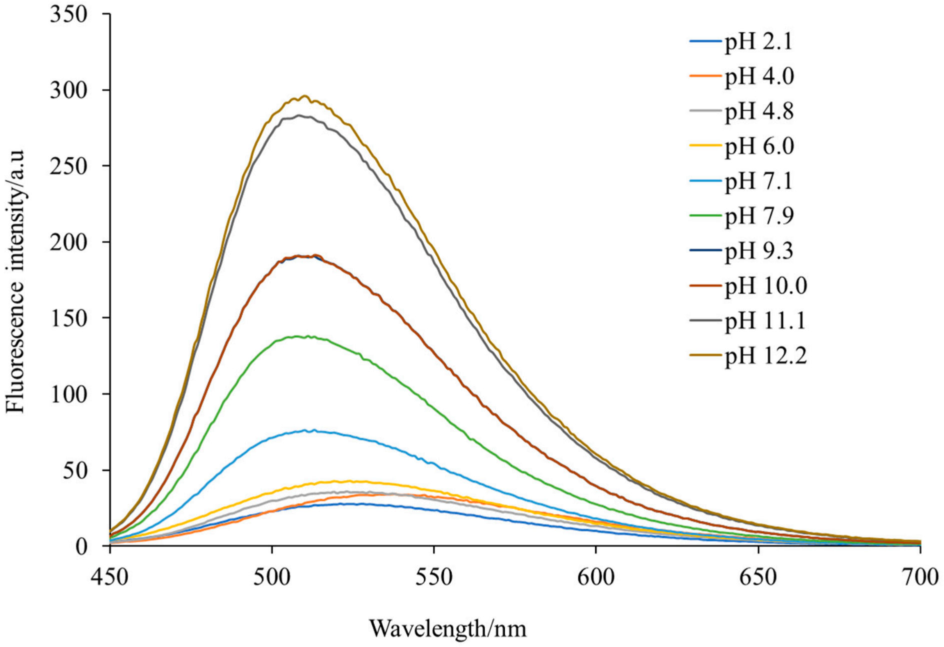

Figure 5. Influence of pH on the fluorescence spectrum of H_3L measured in ethanol at room temperature.

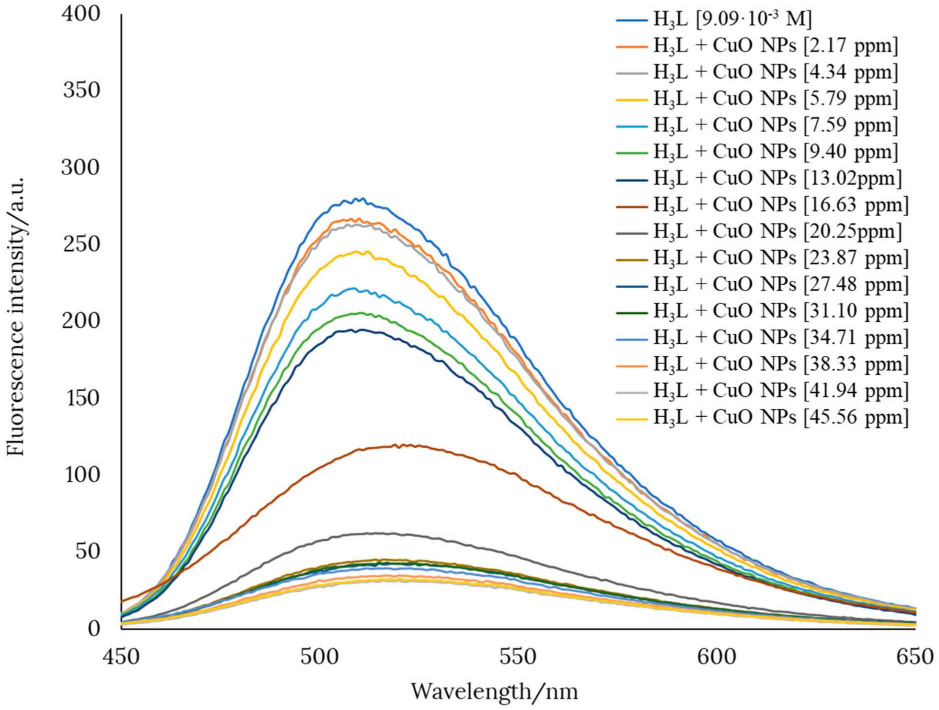

Figure 6. Variation of the fluorescence intensity of an ethanol solution of H_3L after the addition of CuO nanopowder.

3. Conclusions

In conclusion, we can say that we synthetized and characterized a dansyl-based fluorescent ligand that deserves to be explored as a probe for detecting heavy-metal-based nanomaterials in aqueous solution.

4. Experimental Section

Materials and Methods

All starting materials and reagents were commercially available and were used without further purification. ^{1}H-NMR spectra (400 MHz) were measured in deuterated chloroform. J values are given in Hertz. The spectra of the samples were recorded using an ATR-FTIR spectrometer (Spectrum Two, Spectrometer FT-IR UATR, PerkinElmer, Waltham, MA, USA).

N-(2-aminobenzyl)-5-(dimethylamino)naphthalene-1-sulfonamide

The compound was prepared in a 250 mL round flask dissolving 2.35 mmol (0.6339 g) of dansyl chloride in 60 mL of CH_2Cl_2. In a second flask 2.59 mmol (0.3162 g) of 2-aminobenzylamine was dissolved in 40 mL of CH_2Cl_2, to which 2.59 mmol (0.2621 g) of triethylamine were added. This second solution was added in the first-round flask and stirred for 18 h at reflux temperature. It was evaporated to 1/3 of its volume under vacuum and a small portion of diethyl ether was added until the solution became cloudy. After this, it was necessary to filtrate under vacuum and wash with deionized water to separate the triethylamine hydrochloride that was present. The yellow solid was air-dried and weighed to calculate the final yield.

Yield: 0.604 g (75%). ^{1}H NMR (400 MHz, chloroform-*d*, δ in ppm): δ 8.57 (d, *J* = 8.5 Hz, 1H), 8.29 (t, *J* = 8.8 Hz, 2H), 7.57 (t, *J* = 8.3 Hz, 1H), 7.54 (t, *J* = 8.6 Hz 1H), 7.20 (d, *J* = 7.5 Hz, 1H), 7.05 (t, *J* = 7.7 Hz, 1H), 6.80 (d, *J* = 7.4 Hz, 1H), 6.58 (d, *J* = 7.6 Hz, 1H), 6.57 (t, *J* = 7.0 Hz, 1H), 4.77 (t, *J* = 6.1 Hz, 1H), 3.93 (d, *J* = 7.1 Hz, 2H), 2.91 (s, 6H). UV–Vis (ethanol, 4.02×10^{-5} M, λ in nm) 254, 294, 346. Fluorescence λ/nm: λ_{em} 520 (λ_{ex} 340). ATR-FTIR (ν in cm^{-1}): 3472 w (ν_{as} HNH), 3384 m, sh (ν_s HNH), 3323 m (ν NH), 1632 m (δ HNH), 1309 s (ν_{as} OSO), 1143 s (ν_s OSO)

H_3L

The compound was obtained in a 250 mL round flask dissolving the compound *N*-(2-aminobenzyl)-5-(dimethylamino)naphthalene-1-sulfonamide (0.09 g, 0.25 mmol) in $CHCl_3$ (20 mL). Then, while the magnetic stirring was on, a solution of 4-formyl-3-hydroxybenzoic acid (0.0294 g, 0.25 mmol) was added in a molar ratio of 1:1 along with 20 mL $CHCl_3$. A yellow-orange mixture was obtained and then the reflux was switched on for 8 h, using a modified Dean-Stark. During this time, the state of the reaction was monitored by TLC (using a mixture of hexane and ethyl acetate with a 60:40 ratio as eluent). After the 8 h, the yellow-orange solution was concentrated in the rotary evaporator to dryness and a light orange precipitate was obtained. Then, 10 mL of diethyl ether were added to the precipitate and the resulting suspension was left to stir for 6 h. After this time, it was filtered under vacuum and an orange-colored precipitate was obtained, which was left to dry in the oven for a couple of hours. The ether fraction corresponds to impurities that were present.

Yield: 0,099 g (78%); ^{1}H NMR (400 MHz, chloroform-*d*) δ 8.39 (d, *J* = 8.4 Hz, 1H), 8.07 (d, *J* = 9.6 Hz, 2H), 8.05 (d, *J* = 6.9 Hz, 1H), 8.04 (s, 1H), 7.66 (s, 1H), 7.65 (d, *J* = 8.6, 1H), 7.39–7.26 (m, 3H), 7.24 (d, 1H), 7.18 (t, *J* = 7.3 Hz, 1H), 7.11 (d, *J* = 7.4 Hz, 1H), 7.07 (t, *J* = 7.6 Hz, 1H), 6.77 (d, *J* = 7.6 Hz, 1H), 5.15 (t, *J* = 5.6 Hz, 1H), 4.36 (d, *J* = 5.8 Hz, 2H), 2.88 (s, 6H). UV–Vis (ethanol, 10^{-5} M, λ in nm) 224, 248, 340; Fluorescence λ/nm: λ_{em} 546 (λ_{ex} 400). ATR-FTIR (ν in cm^{-1}): $\nu(NH)_{sulfonamide}$ 3283, ν(C=O) 1686, $\nu(C{=}N_{imine})$ 1613, $\nu_{as}(SO_2)$ 1317, $\nu_s(SO_2)$ 1146.

Author Contributions: Conceptualization, J.S.-M. and P.B.-B.; methodology, Y.A.-I.; software, A.M.G.-D. and Y.A.-I.; validation, M.F.; formal analysis, M.F.; investigation, Y.A.-I.; resources, M.F.; data curation, A.M.G.-D.; writing—original draft preparation, J.S.-M.; writing—review and editing, J.S.-M.; visualization, A.M.G.-D. and M.F.; supervision, J.S.-M. and P.B.-B.; project administration, P.B.-B.; funding acquisition, P.B.-B. All authors have read and agreed to the published version of the manuscript.

Funding: Financial support was provided by the Ministerio de Ciencia, Investigación e Universidades (RTI2018-099222-B-I00) and Interreg Atlantic Area, POCTEP.

Acknowledgments: The authors thanks QUIMAOR led by J.M Vila-Abad (GI-1581, USC) for access to the ATR-FTIR instrument.

Conflicts of Interest: The authors declare no conflict of interest.

References

1. Laborda, F.; Bolea, E.; Cepria, G.; Gómez, M.T.; Jiménez, M.S.; Pérez-Arantegui, J.; Castillo, J.R. Detection, characterization and quantification of inorganic engineered nanomaterials: A review of techniques and methodological approaches for the analysis of complex samples. *Anal. Chim. Acta* **2016**, *904*, 10–32. [CrossRef] [PubMed]
2. Yan, A.; Chen, Z. Detection methods of nanoparticles in plant tissues. In *New Visions in Plant Science*; Çelik, Ö., Ed.; Intechopen: London, UK, 2018; Chapter 6.
3. Navratilova, J.; Praetorius, A.; Gondikas, A.; Fabienke, W.; Kammer, F.; Hofmann, T. Detection of engineered copper nanoparticles in soil using single particle ICP-MS. *Int. J. Environ. Res. Public Health* **2015**, *12*, 15756–15768. [CrossRef] [PubMed]
4. Medina-Sánchez, M.; Miserere, S.; Marín SAragay, G.; Merkoçi, A. On-chip electrochemical detection of CdS quantum dots using normal and multiple recycling flow through modes. *Lab. Chip* **2012**, *12*, 2000–2005. [CrossRef] [PubMed]
5. Chatterjee, A.; Santra, M.; Won, N.; Kim, S.; Kim, J.K.; Kim, S.B.; Ahn, K.H. Selective fluorogenic and chromogenic probe for detection of silver ions and silver nanoparticles in aqueous media. *J. Am. Chem. Soc.* **2009**, *131*, 2040–2041. [CrossRef] [PubMed]
6. Cayuela, A.; Soriano, M.L.; Valcárcel, M. Reusable sensor based on functionalized carbon dots for the detection of silver nanoparticles in cosmetics via inner filter effect. *Anal. Chim. Acta* **2015**, *872*, 70–76. [CrossRef] [PubMed]
7. Rebe Raz, S.; Leontaridou, M.; Bremer, M.G.E.G.; Peters, R.; Weigel, S. Development of surface plasmon resonance-based sensor for detection of silver nanoparticles in food and the environment. *Anal. Bioanal. Chem.* **2012**, *403*, 2843–2850. [CrossRef] [PubMed]
8. Sanmartín-Matalobos, J.; García-Deibe, A.M.; Fondo, M.; Zarepour-Jevinani, M.; Domínguez-González, M.R.; Bermejo-Barrera, P. Exploration of an easily synthesized fluorescent probe for detecting copper in aqueous samples. *Dalton Trans.* **2017**, *46*, 15827–15835. [CrossRef]
9. Sanmartín-Matalobos, J.; García-Deibe, M.; Zarepour-Jevinani, M.; Aboal-Somoza, M.; Bermejo-Barrera, A.M.; Fondo, P. Exploring the Chelating Potential of an Easily Synthesized Schiff Base for Copper Sensing. *Crystals* **2020**, *10*, 235. [CrossRef]
10. Srivastava, P.; Ali, R.; Razi, S.S.; Shahid, M.; Patnaik, S.; Misra, A. A simple blue fluorescent probe to detect Hg^{2+} in semiaqueous environment by intramolecular charge transfer mechanism. *Tetrah. Lett.* **2013**, *54*, 3688–3693. [CrossRef]
11. Van Beijnen, A.J.M.; Nolte, R.J.M.; Naaktgeboren, A.J.; Zwikker, J.W.; Drenth, W. Helical Configuration of Poly (iminomethylenes). Synthesis and CD spectra of Polymers derived from optically active isocyanides. *Macromolecules* **1983**, *16*, 1679–1689. [CrossRef]